Supporting Information

Liang et al. 10.1073/pnas.1721868115

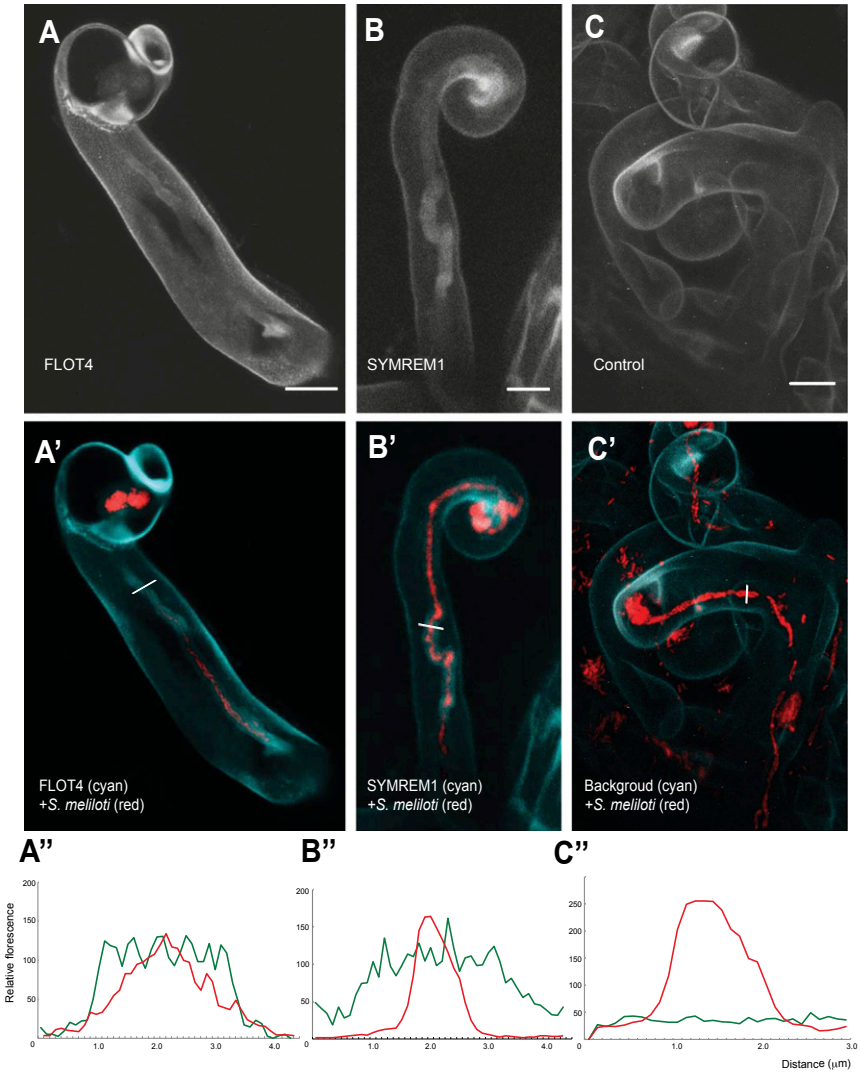

Fig. S1. Comparison of fluorescent background levels around ITs in the immunofluorescence assay. (*A* and *B*) Immunofluorescence targeting FLOT4-GFP (*A*–*A*″) and GFP-SYMREM1 (*B*–*B*″), both expressed from their endogenous promoters. (*C*–*C*″) As a control, the same immunofluorescence protocol was applied to nontransformed but infected root hairs from the same batch of samples. *A*, *B*, and *C* show the GFP channel; *A*′, *B*′, and *C*′ show the merged channel with *S. meliloti* 2011 (mCherry) infection. The lines in *A*′, *B*′, and *C*′ indicate transects used for the relative florescence analysis displayed below. *A*″, *B*″, and *C*″ indicate the florescent gray value, in which red represents the value of the mCherry channel and green represents the GFP channel. *A* and *A*′ and *B* and *B*′ are identical to Fig. 1. (Scale bars: 10 μm.)

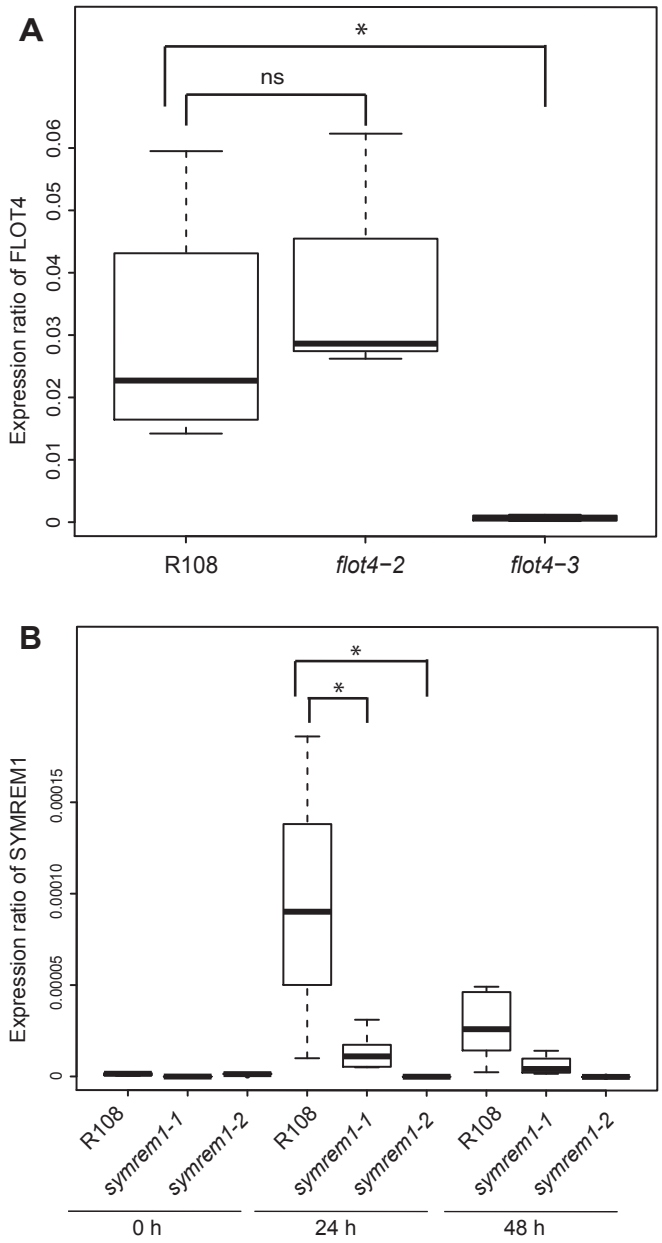

Fig. S2. Determining transcript and protein levels in *Tnt1* insertion lines. (*A*) *FLOT4* transcript levels in *flot4-2* and *flot4-3* insertion lines and WT R108 plants. (*B*) *SYMREM1* transcript level before inoculation and at 24 h and 48 h postinoculation in *symrem1-1* and *symrem1-2* mutant lines. Quantitative RT-PCR (qRT-PCR) was performed on cDNA obtained from roots, with five biological replicates. The graphs represent the ΔΔCt values obtained by qRT-PCR in relative to ubiquitin. *$P < 0.05$ obtained from the Student *t* test in *A* and from the Dunnett multiple- comparison test in *B*. ns, not significant.

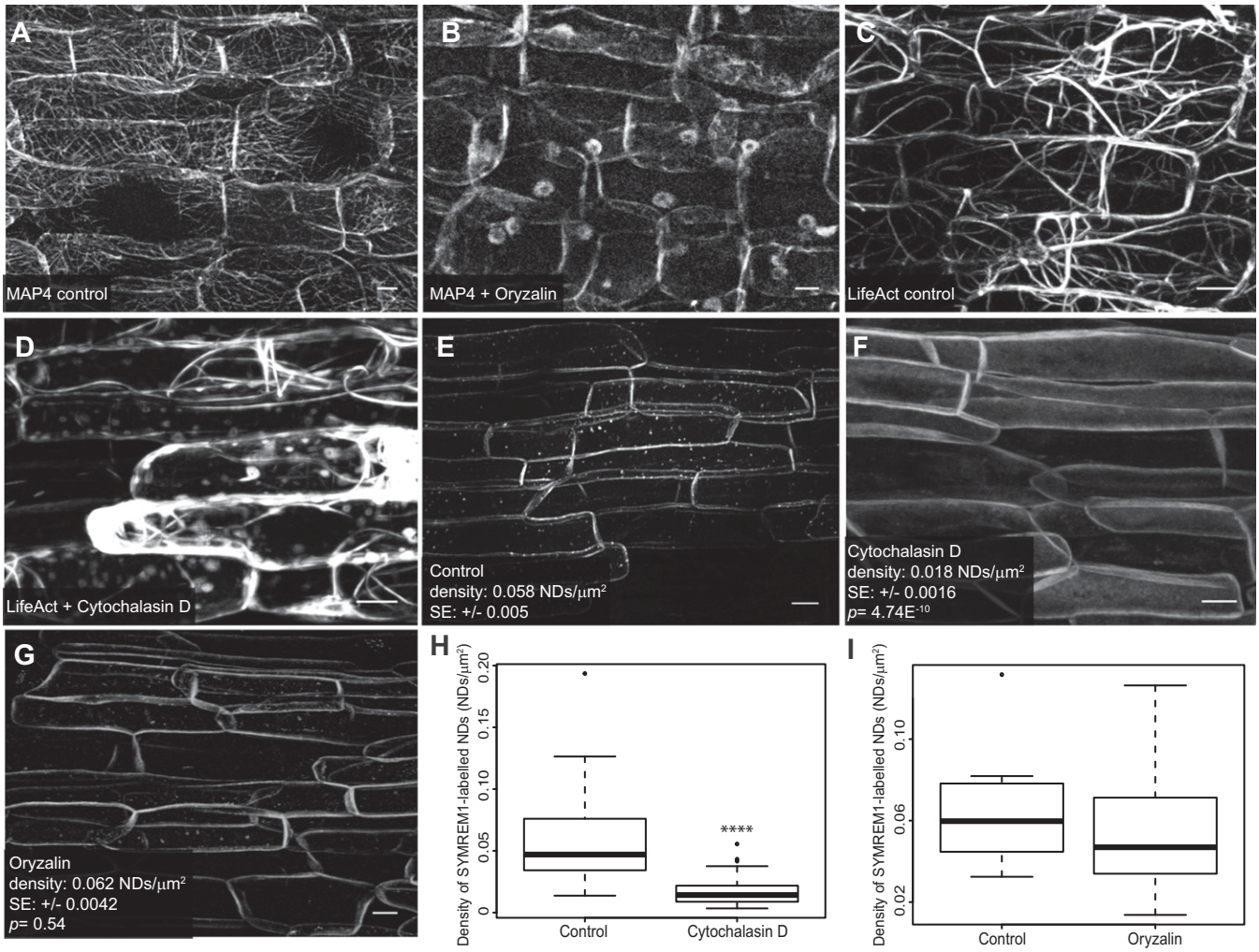

Fig. S3. Recruitment of SYMREM1 into nanodomains (NDs) is actin-dependent. (*A–D*) The efficiency of drug application to destabilize microtubules (*A* and *B*) and actin (*C* and *D*) was tested by applying oryzalin (*B*) and cytochalasin D (*D*) on roots expressing fluorophore-tagged MICROTUBULE-ASSOCIATED PROTEIN 4 (MAP4) (*A* and *B*) or Lifeact (*C* and *D*). (*E–I*) The density of YFP-SYMREM1–labeled nanodomains was significantly higher in control roots (*E* and *H*) compared with roots treated with cytochalasin D (*F* and *H*), while depolymerizing microtubules (*G* and *I*) did not change YFP-SYMREM1 localization. Quantitative image analysis was performed on all samples as indicated below the individual panels. ****$P < 0.0001$ obtained from Student *t* tests. (Scale bars: 10 μm.)

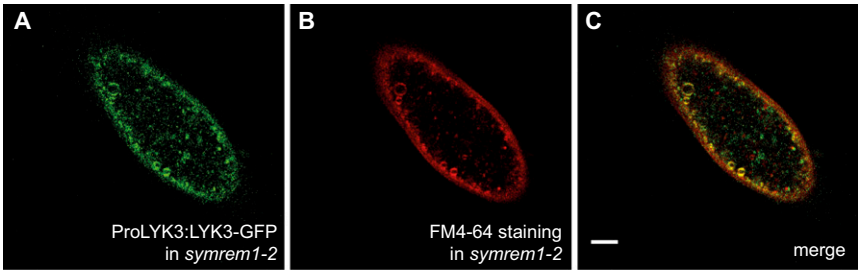

Fig. S4. Activated LYK3 receptor localizes to endosomes in *symrem1-2* mutants on prolonged rhizobial inoculation. (*A*) ProLYK3:LYK3-GFP was expressed in *symrem1-2* mutant roots and imaged in root hairs at 2 dpi with *S. meliloti*. (*B* and *C*) To test the plasma membrane origin of the observed vesicles, samples were counterstained with FM4-64 (*B*), and images were subsequently merged (*C*). (*D*) Fluorescence intensity plot of a representative transect (position indicated in *C*) showing a high degree of colocalization in these structures. (Scale bar: 5 μm.)

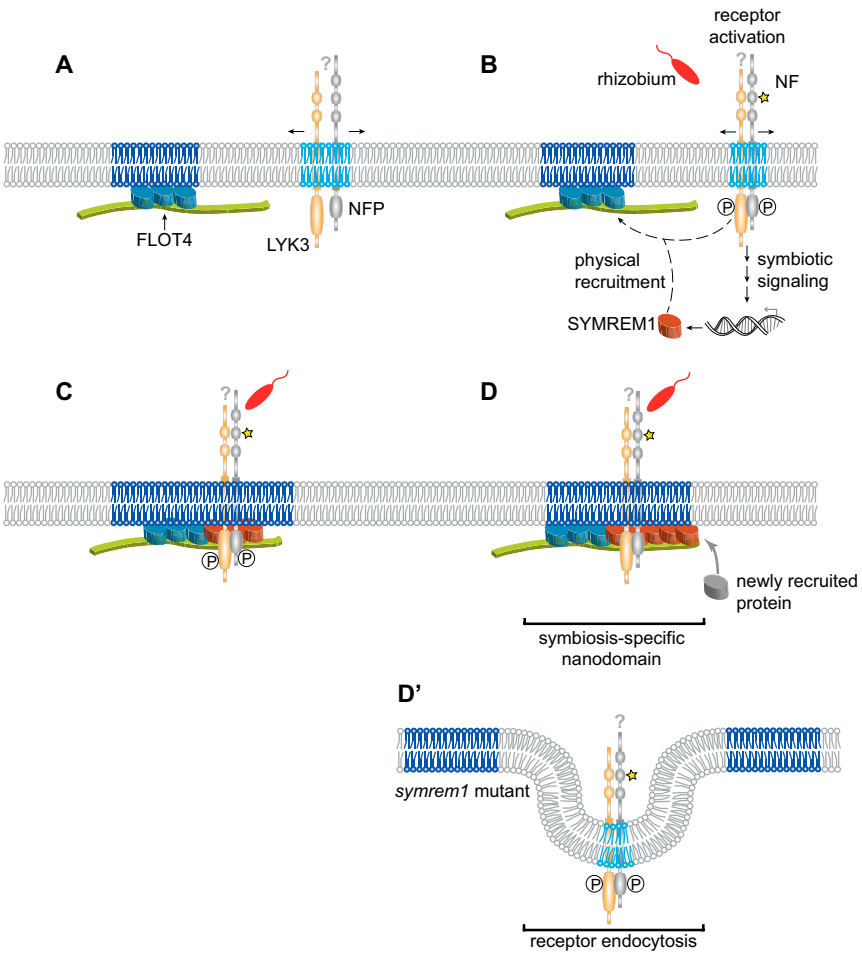

Fig. S5. Proposed model for nanodomain assembly. (*A*) Constitutively expressed FLOT4 (turquoise) forms a primary nanodomain scaffold that is unable to recruit LYK3 in the absence of SYMREM1. (*B*) Nod factor (NF) perception by NFP (gray) and LYK3 (orange) occurs in mobile nanodomains and results in the activation of a symbiosis-specific signaling cascade that leads to the expression of *SYMREM1* (red). (*C*) Due to its ability to directly bind LYK3 (1), SYMREM1 actively recruits the receptor into the FLOT4 nanodomain. (*D*) Phosphorylation of SYMREM1 by LYK3 may trigger remorin oligomerization, which generates new docking sites for proteins required for rhizobial infection (hypothetical). (*D'*) In *symrem1* mutants, LYK3 is destabilized and endocytosed on rhizobial inoculation.

1. Lefebvre B, et al. (2010) A remorin protein interacts with symbiotic receptors and regulates bacterial infection. *Proc Natl Acad Sci USA* 107:2343–2348.

Table S1. Quantification of LYK3 mobility

Mobility	Uninoculated	*S. meliloti* (2 dpi)	ProUbi:YFP-SYMREM1
>180 s	1/20	9/9	30/49
60–180 s	—	—	16/49
<30 s	19/20	—	3/49

Values are frequencies of categories detected in a set of observed root hairs (n = 9–49). Pixel dwell times of LYK3-labeled nanodomains were categorized as >180 s, 60–180 s, and <30 s.

Table S2. Primers used in the study

Primer	Sequence (5′-3′)	Used for	References or referenced ID
FLOT2-F1	AGTCAGAGTCCCTCGCCAGTACAAT	Genotyping	Medtr3g106420
FLOT2-R1	CAAGAAATACCAAGCACGTAAAGACATAAT	Genotyping	Medtr3g106420
FLOT2-F2	GAGAGCTGGAGAGGGTGAGAA	Genotyping	Medtr3g106420
FLOT2-R2	GACTTGCAAAAACTACAATGTGACGTTA	Genotyping	Medtr3g106420
FLOT2-F3/4	AGAAACAGAAAGAGACTGAAGCAATTC	Genotyping	Medtr3g106420
FLOT2-R3	CCAGCAACTTCTTTCATACCCAT	Genotyping	Medtr3g106420
FLOT2-R4	CATCATCCTAATCAAGAGCTTTTCTCA	Genotyping	Medtr3g106420
FLOT4-F	CCTTCCATACCATACACCTTACACCAT	Genotyping	Medtr3g106430
FLOT4-R	CACCCCCACTATTATCACCACCATTAGT	Genotyping	Medtr3g106430
TNT1-F	GTAGAGAATAGGTAAGGTGCT	Genotyping	(1)
TNT1-R	TGTAGCACCGAGATACGGTAATTAACAAGA	Genotyping	(1)
TNT1-R1	TGTAGCACCGAGATACGGTAATTAACAAGA	Genotyping	(1)
SYMREM1-F	CCCAATATATACATGTCCTC	Genotyping	Medtr8g097320
SYMREM1-R	CCAAAACAAGCAAGCTAATGAA	Genotyping	Medtr8g097320
Ubi-F	TTGTGTGTTGAATCCTAAGCA	Housekeeping gene for qRT-PCR	(2)
Ubi-R	CAAGACCCATGCAACAAGTTC	Housekeeping gene for qRT-PCR	(2)
qFLOT4-F	TACACTGCTGTAAGGGATTTC	qRT-PCR	Medtr3g106430
qFLOT4-R	CTTTCATCGCACCTTCACC	qRT-PCR	Medtr3g106430
qSYMREM1-F	GTGGGAGGATGATAAGAAAGC	qRT-PCR	Medtr8g097320
qSYMREM1-R	CTGATAGCCACGAGTACGAAA	qRT-PCR	Medtr8g097320

1. Tadege M, et al. (2008) Large-scale insertional mutagenesis using the Tnt1 retrotransposon in the model legume *Medicago truncatula*. *Plant J* 54:335–347.
2. Satgé C, et al. (2016) Reprogramming of DNA methylation is critical for nodule development in *Medicago truncatula*. *Nat Plants* 2:16166.

Table S3. Gene constructs used in this study

Construct cassette	Method	Backbone	Used for	GenBank accession no. or reference
ProSYMREM1-GW	Gateway	pUB-GW(HYG)	Cloning	JQ061257
ProSYMREM1:NLS-2xGFP	Golden Gate LII	L2βF1-2	Expression pattern	JQ061257
ProFLOT4:NLS-2xGFP	Golden Gate LII	L2βF1-2	Expression pattern	CT009553
ProSYMREM1:GFP-SYMREM1	Golden Gate LII	L2βF1-2	LIII construct module	JQ061257
ProFLOT4:FLOT4-GFP	Golden Gate LII	L2βF1-2	LIII construct module	GU224281
ProUbi:GFP-SYMREM1	Golden Gate LII	L2βR1-2	Nanodomain quantification	JQ061257
ProUbi:FLOT4-GFP	Golden Gate LII	L2βR1-2	Nanodomain quantification	GU224281
ProUbi:NLS-2xCerulean	Golden Gate LII	L2βR 5–6	LIII construct module as prescreen marker	(1)
ProSYMREM1:GFP-SYMREM1//ProUbi:NLS-2xCerulean	Golden Gate LIII	L3βF A-B	Localization	JQ061257
ProFLOT4:FLOT4-GFP//ProUbi:NLS-2xCerulean	Golden Gate LIII	L3βF A-B	Localization	GU224281
ProUbi:FLOT4:RNAi	Golden Gate LII	L2βRNAi F1-2	FLOT4 gene silencing	GU224281
ProUbi:YFP-MAP4	Golden Gate LII	L2βF1-2	Microtubule marker	M72414
ProUbi:YFP-Lifeact	Golden Gate LII	L2βF1-2	Actin marker	(2)

1. Binder A, et al. (2014) A modular plasmid assembly kit for multigene expression, gene silencing and silencing rescue in plants. *PLoS One* 9:e88218.
2. Bücherl CA, et al. (2017) Plant immune and growth receptors share common signalling components but localise to distinct plasma membrane nanodomains. *eLife* 6:e25114.